Safety Verification of Seismic Isolation System using Sliding Bearings against Long Period Earthquake Motions

H. Hibino, R. Maseki & A. Nii
Technology Center, Taisei Corporation, Kanagawa, Japan

S. Minewaki, M. Yamamoto & H. Yoneda
Research and Development Institute, Takenaka Corporation, Chiba, Japan

M. Takayama
Fukuoka University, Fukuoka, Japan

M. Kikuchi
Hokkaido University, Hokkaido, Japan

M. Iiba
Building Research Institute, Ibaraki, Japan

SUMMARY:
Long-period ground motions with large amplitudes are expected to occur in Japan in the near future, and they may have a considerable impact on seismic-isolated buildings. Therefore, it is important to verify the safety of such buildings against long-period ground motions. This paper describes the results of multicyclic loading tests of sliding bearings used for seismic isolation. High-friction bearing specimens showed increasing temperatures and decreasing friction coefficients according to loading cycles, and the trend of fluctuation of friction correlated well with such parameters as cumulative absorbed energy. Low-friction bearings showed extremely low fluctuation even under additional axial pressure; however, the trend of friction fluctuation, such as in terms of the fluctuation range or recovery, that was observed in the tests could not be expressed through conventional estimation. Both types of sliding bearings showed sufficient stability against multicyclic loading under the test conditions considering seismic responses.

Keywords: Seismic isolation, Long-period earthquake motion, Sliding bearing

1. INTRODUCTION

In the recent years, long-period earthquake motions caused by subduction zone earthquakes around Japan and their impact on super high-rise buildings and base-isolated buildings have attracted great public concern and interest in Japan. In fact, the 2011 off the Pacific coast of Tohoku Earthquake brought about long-period ground motions in the Kanto plain, which shook super high-rise buildings as well as base-isolated buildings for a long duration of more than several minutes. It is expected that Tokai, Tonankai, Nankai, or their coupled earthquakes may occur in the near future, and the Kanto, Nobi, and Osaka plains will be exposed to long-period ground motions with larger amplitudes. It is therefore essential to verify the safety of seismic isolation systems against long-period earthquake motions. To assess the above-mentioned issue, we conducted multicyclic loading tests of both high-friction and low-friction small-scale sliding bearings.

2. TESTS OF HIGH-FRICTION SLIDING BEARINGS

2.1. Objective

The objective of the multicyclic loading tests described here was to investigate the trend of the fluctuation of characteristics and marginal performance of high-friction elastic sliding bearings.

With regard to the multicycle characteristics of these bearings, many experimental studies have been carried out to estimate the effect of loading cycles on friction using polytetrafluoroethylene (PTFE) sliding bearing specimens (Hibino et al., 2003). These studies generally indicate that the friction of sliding bearings decreases with an increase in the number of loading cycles, and that it tends to vary with the temperatures of the sliding plate and bearing as well as the cumulative absorbed energy.

2.2. Specimens

The tests used 5 specimens of sliding bearings with diameters of 300 mm, which were one-third the size of a full-size bearing. The sliding material of the bearing was PTFE, whose dynamic friction coefficient (μ, which is hereafter used to denote the friction coefficient) with the SUS plate was 0.10, and its standard axial pressure was 20 MPa. The tests also used 2 sets of sliding plates that consisted of thick steel base plates and thin SUS surface plates. Drawings of a specimen with the layout of thermal measurement points are shown in Fig. 2.1.

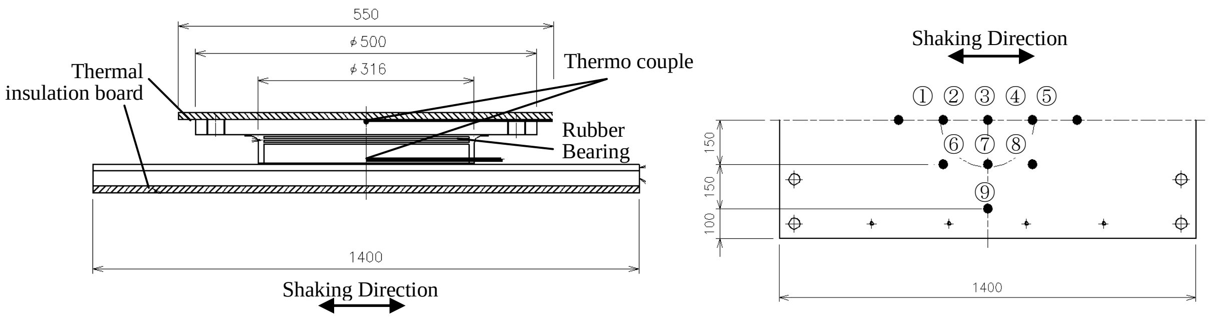

Thickness of rubber: 2.5mm
Number of rubber layers: 3
S1 = 30, S2 = 40, μ = 0.10, CR

SUS304(t9) + SS400(t22)

(Thermal measurement points are also shown)

Sliding bearing

Sliding plate

Figure 2.1 High-friction sliding bearing and sliding plate specimens

2.3. Test Conditions

A dynamic biaxial testing machine was used for the tests. In each test, a one-dimensional dynamic shear loading was conducted under a constant axial force. The axial force with an axial pressure of 20 MPa was set as the default, and tests under a doubled axial force were also conducted. Sinusoidal loading tests with period of 4 s were conducted as the basic case. The number of cycles for the long-period test was determined as the total number of shear displacements that might exceed 50 m, which was assumed to exceed the actual number during a single earthquake with long-period ground motions. The number of cycles for the finite tests was doubled for long-period tests. A “set” was determined by the available continuous loading cycles of the machine specifications, and time intervals of approximately 3 min were inserted into every set. In several cases, tests were conducted through to completion without any time intervals.

Seismic loading tests with displacement response of a base-isolated mass (yield base shear of 0.03 and period of 4 s) were also conducted, which were simulated from the generated input motion of coupled Tokai, Tonankai, and Nankai earthquakes. The input motion data were provided by the results from Shimizu Corporation (2010). Table 2.1. lists the test cases.

The measured data were horizontal displacement, horizontal force, axial force, and temperature. The temperature was measured on the sliding plate, on the backplate of the sliding bearing, on the lateral face of the rubber block, and in the atmosphere.

Table 2.1. Test cases

No.	Case		Surface pressure (MPa)	Displacement (mm)	Number of cycles	Total amount of displacement (m)
1	Long-period	1A-1	20	100	125 †	50
		1A-2				50
	Ultimate	1B			250 [w/o intervals]	100
2	Ultimate	1B			250 ††	100
3	Ultimate	2B		200	125†	100
4	Long-period	1A-1	40	100	125†	50
		1A-2				
5	Seismic	AIC003-AV	20	210	-	-
	Ultimate	3B		230	100 †††	92
		1B	40	100	250 [w/o intervals]	100

†40 cycles × 3 sets + 5 cycles, ††40 cycles × 6 sets + 10 cycles, †††15 cycles × 6 sets + 5 cycles × 2 sets

2.4. Test Results

The relationships between the friction coefficient (horizontal force divided by axial force) and displacement from the multicyclic loading tests are shown in Fig. 2.2. As also shown in Figs. 2.3 and 2.4, the friction coefficient of the bearing surfaces decreased with increasing loading cycles. The changing rate of friction from initial for #1:1A and #1:1B (w/o intervals) were −59% and −67%, respectively. A relationship between the horizontal force and displacement from the seismic loading test is shown in Fig. 2.5. The average axial force at the displacement origin for each cycle decreased gradually with loading. As shown in Fig. 2.3, the friction coefficient gradually recovered (increased) during the time intervals.

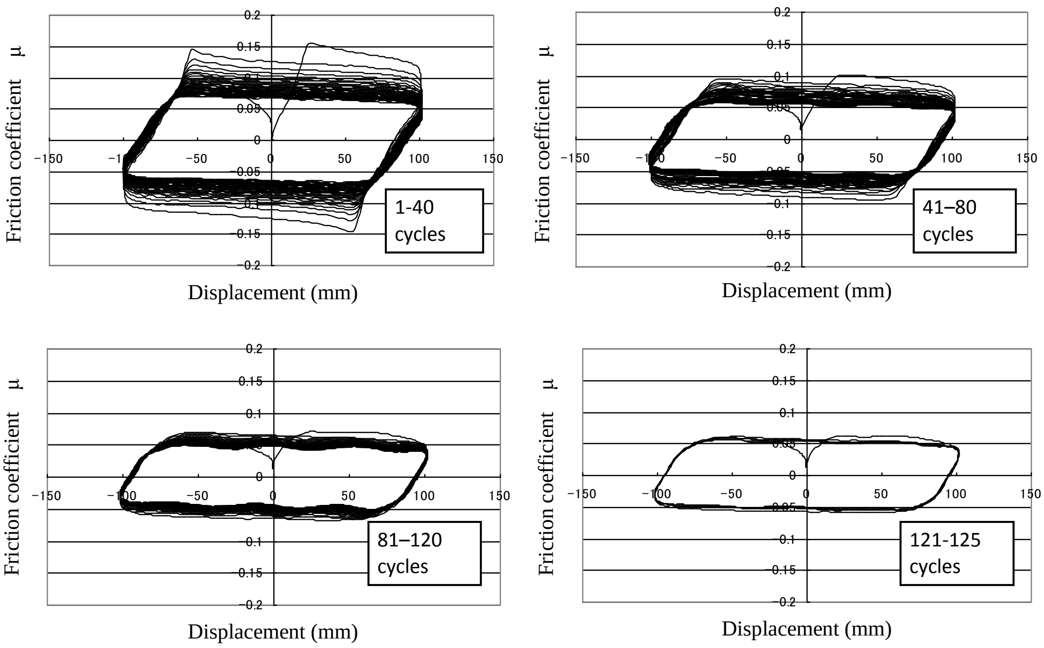

Figure 2.2 Relationship between horizontal force and displacement
(#1:1A-1, Long-period)

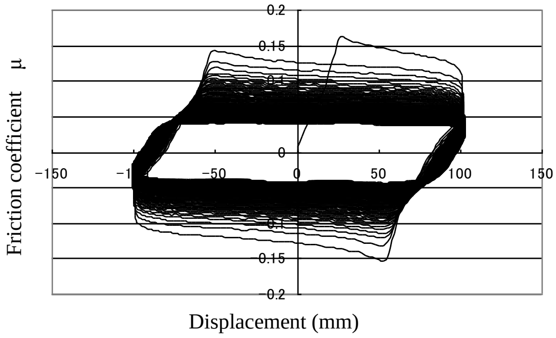

Figure 2.3 Relationship between horizontal force and displacement
(#1:1B-Ultimate [w/o intervals])

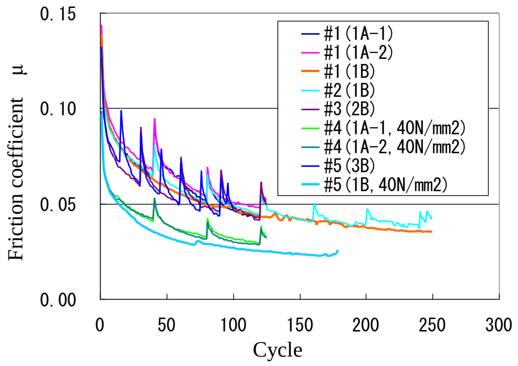

Figure 2.4 Relationship between friction coefficient and cycle number

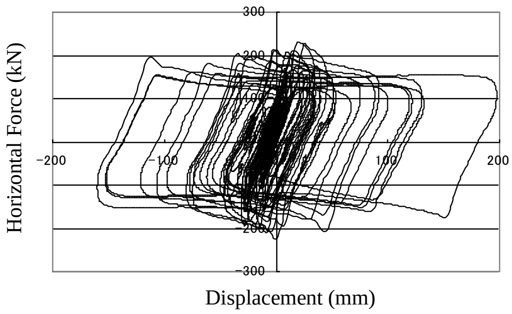

(#5: Seismic, AIC003-AV)

Figure 2.5 Relationship between horizontal force and displacement

The friction coefficient is assumed to decrease because of frictional heating, which causes the friction coefficient of the bearing surfaces to decrease with loading cycles, and the coefficient gradually recovers during the loading interval. With that, single regression analysis was performed on the friction coefficient with the parameters of the temperature of the sliding plate, cumulative absorbed energy, and cumulative bearing displacement. The results of logarithmic regression are shown in Figs. 2.6 and 2.7, and the friction coefficient is well correlated with each parameter.

For seismic response analysis, a friction characteristics model was formulated according to Eqn. 2.1 and Fig. 2.8, and multi-regression analysis of the friction coefficient was carried out for Case #1:1B-Ultimete [w/o intervals]. Here, cumulative sliding displacement was used in place of the bearing displacement on the assumption that frictional heating causes a decrease in friction.

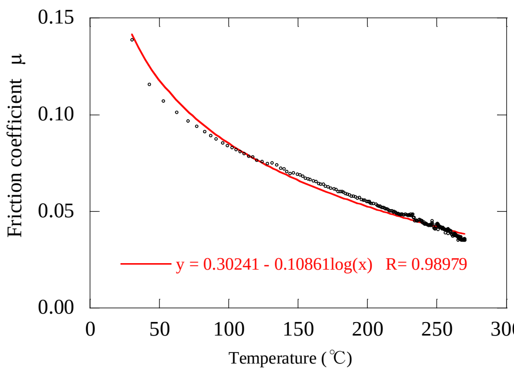

Figure 2.6. Relationship between friction coefficient and temperature of the sliding plate
(#1:1B-Ultimete [w/o intervals])

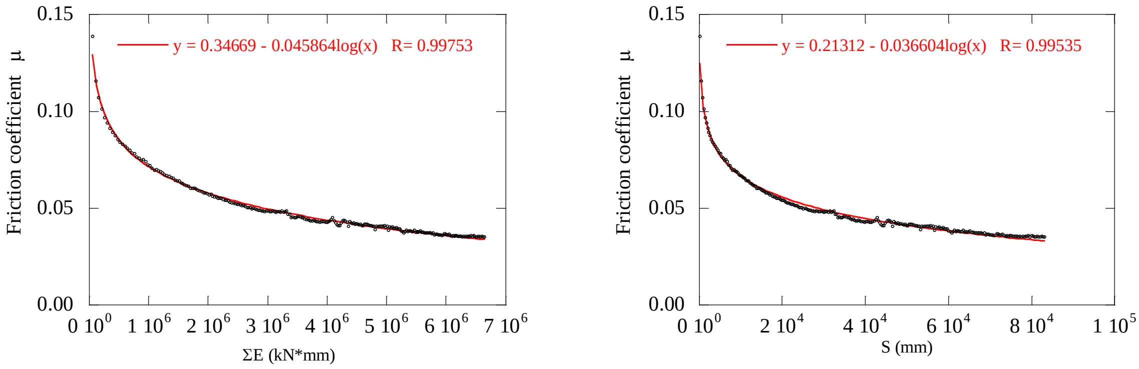

Cumulative absorbed energy Cumulative sliding displacement

Figure 2.7 Relationship between friction coefficient and each parameter (#1:1B-Ultimete [w/o intervals])

$$\mu(t) = a \cdot (\log v(t) - \log v_0) \cdot (\log E(t) - \log E_0) + b \tag{2.1}$$

Here, a, b, v_0, and E_0 are the constants, and μ(t), v(t), and E(t) are the time function of the friction coefficient, velocity, and cumulative absorbed energy, respectively. Constants obtained from the regression of a test case (#1:1B) are listed in Table 2.2.

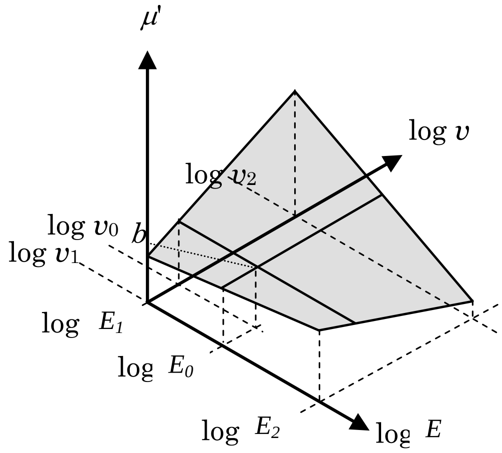

Figure 2.8 Friction characteristics model

Table 2.2. Parameters of Eq.2.1 obtained from multi-regression

Surface pressure σ (MPa)	Parameters				Range of data			
					v (cm/s)		E (kN·mm)	
	a	b	v_0 (cm/s)	†E_0 (kN·mm)	lower limit v_1	upper limit v_2	lower limit †E_1	upper limit †E_2
20	–2.575E–02	1.086E–01	2.546E–01	1.638E+05	15	37	7.600E+02	6.643E+06

† value for the specimen of φ300 and for the surface pressure 20MPa; it should be multiplied by the magnifications of axial force

As the result of the tests, the temperature of the sliding plate and bearing surface gradually increased with increasing loading cycles as shown in Fig. 2.9. The temperatures on the surface of the sliding plate for the #1:1A-1, 1A-2, and #2:1B were 236 °C, 238 °C, and 258 °C, respectively. In the case of high-velocity or continuous cyclic loading, the temperatures increased remarkably. For example, temperatures on the surface of sliding plate #3:2B, #5:3B, and #1:1B were 286 °C, 265 °C, and 270 °C, respectively. However, in the seismic loading test, temperatures on the sliding plate and on the lateral face of rubber block were below about 100 °C and near room temperature, respectively.

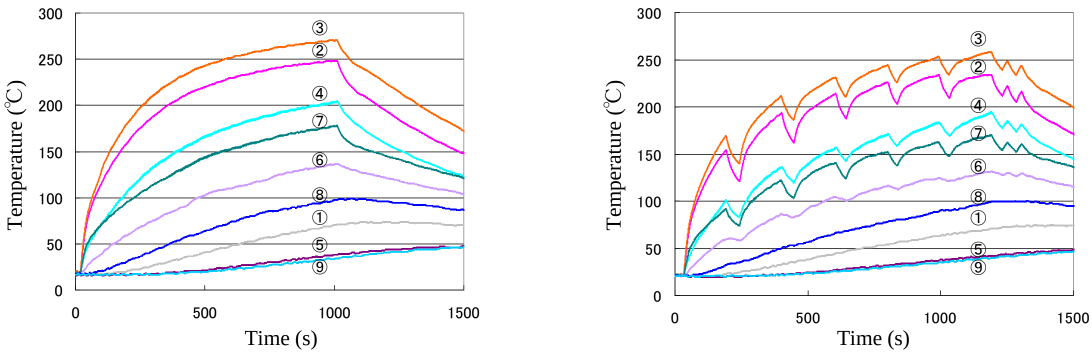

#1:1B-Long-period [w/o intervals]

#2:1B-Ultimate

Figure 2.9 Temperature variation on sliding plate

Any noticeable damage was not observed in Specimen #1 (after 2 long-period tests) and #2 (after the ultimate test). Consequently, the high-friction type sliding bearing was robust against multicyclic loading at an axial pressure of 20 MPa and cumulative displacements of 50 m. At the same time, in all three cases #4:1A-1,1A-2 and #5:1B, under an axial pressure of 40 MPa, cold flow and protrusion of the PTFE were observed when the sliding plate temperatures exceeded 240 °C. Consequently, it was concluded that the softening of PTFE and high pressure caused these phenomena.

3. TESTS OF LOW-FRICTION SLIDING BEARINGS

3.1. Objective

The objective of the multicyclic loading tests described here was to investigate the trend of fluctuation of characteristics and marginal performance of low-friction elastic sliding bearings. The specimen was a type of verification device for seismic isolation authorized by the Japanese Ministry of Land, Infrastructure and Transport (2008).

In conventional studies of the multicycle characteristics of these bearings (Hamazaki et al., 2007), it has generally been pointed out that the friction coefficient of a sliding bearing increases with an increase in the number of loading cycles. This formulation has been proposed to estimate the variations of the friction coefficient depending on the number of loading cycles.

3.2. Specimens

The tests used 4 specimens of sliding bearings with diameters of 400 mm (sliding materials, 350 mm). The sliding material of the bearing was PTFE with a friction coefficient against the SUS plate of 0.01, and its standard axial pressure was 20 MPa. Small holes filled with solid lubricant were arrayed on the surface of the sliding material. The drafts and the specifications for the specimens are shown in Fig. 3.1 and listed in Table 3.1, respectively.

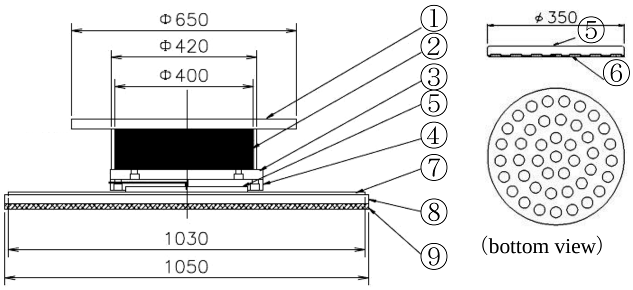

Figure 3.1 Specimen with low-friction sliding bearing and sliding plate

Table 3.1. Specifications for low-friction sliding bearing specimens

No.	Item		Material	Size
①	Upper flange plate		SS400	φ650 × t30
②	Rubber bearing	Rubber	Natural rubber G6	t4 × 9
		Steel plate	SPHC similar	t2.5 × 8
③	Lower flange plate		SS400	φ420 × t30
④	Sliding material holder		SS400	φ420 × t25
⑤	Sliding material		Glass epoxy resin/PTFE	φ350 × t8
⑥	Filling material		Solid lubricant	–
⑦	Sliding plate		SUS304 (Special lubricant coating treatment)	□1030 × t6
⑧	Attachment plate for sliding plate		SS400	□1050 × t16
⑨	Thermal insulation board (thermal conductivity: 0.3W/m/K)		Aluminum carbonate	□1050 × t10

3.3. Test Conditions

In this investigation, the total displacement of an isolated layer because of a single long-period earthquake motion was assumed to be 50 m. The loading relative to this displacement was labeled as a "set". Each specimen was subjected to 10 sets of 4 types of loading conditions with intervals inserted after every set. The test conditions are listed in Table 3.2. A dynamic biaxial testing machine was used for the tests.

Table 3.2. Test Conditions

Specimen No.	Loading waveform	Period (s)	Displacement (mm)	Surface pressure (MPa)	Time interval (min)	Number of cycles	Total amount of displacement (m)
#1	sinusoidal	4	150	20	30	84 × 10	50.4 × 10
#2			50 to 300 (fluctuated†)	20	30	94 × 10	50.6 × 10
#3			150	30	30	84 × 10	50.4 × 10
#4			150	20	3–11††	84 × 10	50.4 × 10

†50 mm → 100 mm → 150 mm → 200 mm (each 11 cycles) → 250 mm → 300 mm (each 3 cycles)
→ 200 mm → 150 mm → 100 mm → 50 mm (each 11 cycles)
††up to the 7^{th} set: 11 min, from 8^{th} set: 3min

3.4. Test Results

The relationship between the friction coefficient and the displacement of the 1^{st} and 10^{th} sets by the multicyclic loading tests are shown in Figs. 3.2–3.5. The displacement was defined as the overall deformation including elastic deformation of the rubber bearing. Except for the 10^{th} set of Specimen #4, a remarkable decrease in the friction coefficient was observed in each set. For Specimens #1 and #2, no significant change was observed between the 1^{st} and the 10^{th} sets. The friction coefficient increased remarkably in Specimen #3, and decreased at the beginning of each set in Specimen #4.

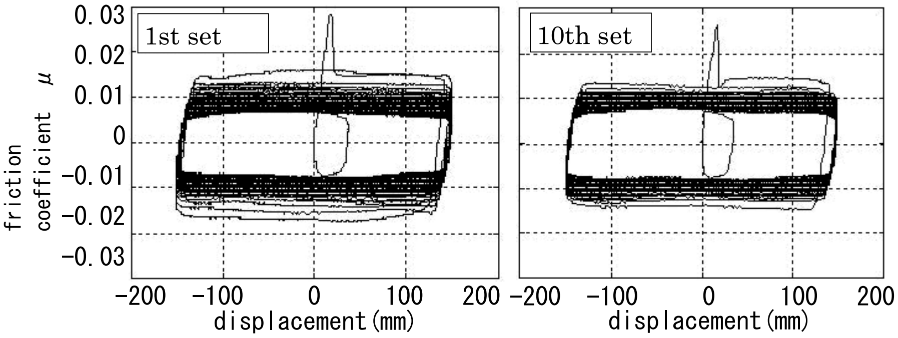

Figure 3.2 Relationship between friction coefficient and displacement (Specimen #1)

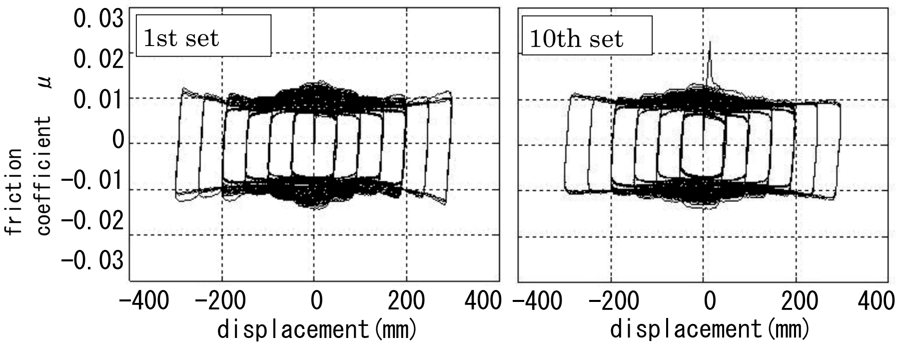

Figure 3.3 Relationship between friction coefficient and displacement (Specimen #2)

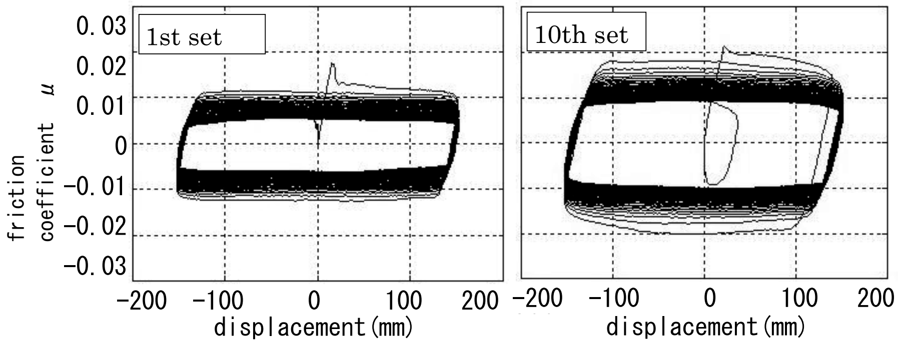

Figure 3.4 Relationship between friction coefficient and displacement (Specimen #3)

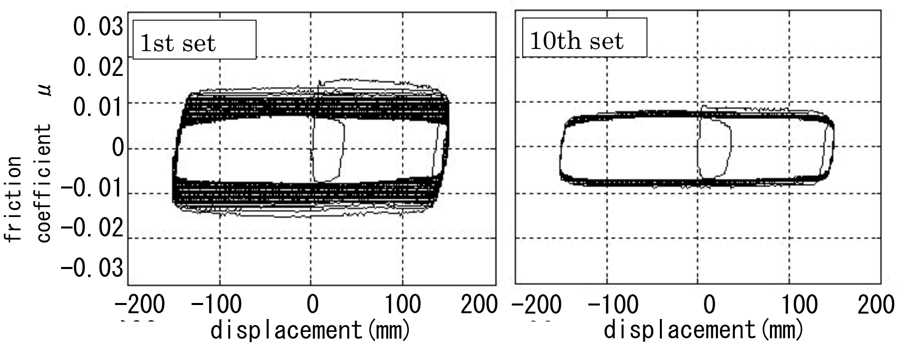

Figure 3.5 Relationship between friction coefficient and displacement (Specimen #4)

Fig. 3.6 shows apparent condition of the sliding plate after the tests of Specimens #1 and #3. On the surface of sliding plate, only a partial scratch is observed in the case of #1, but exposure of the glossy surface and abruption of the coating is observed in the case of #3.

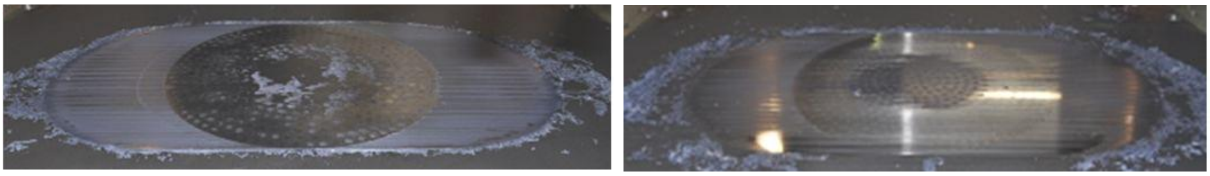

a) Specimen #1 b) Specimen #3

Figure 3.6 Sliding plates after 10 sets of tests

Fig. 3.7 shows the relationship between the friction coefficient obtained as averaged axial force at displacement 0 and the number of loading cycles. The values of the friction coefficient were obtained at a pressure of 20 MPa and a velocity of 15 mm/s. Several data results based on conventional studies are also shown in the figure. For each specimen, the friction coefficient drops rapidly at the beginning of each set, and it gradually becomes steady. As for the friction coefficient at the beginning of each set, those values were almost same in every set of Specimens #1 and #2, and up to the 5th set of Specimen #3; then, they gradually declined in Specimen #4. In addition, the friction coefficient at the end of each set showed only slight difference in each set of Specimens #1, #2, and #4, whereas it began to rise for the 6th set in Specimen #3, after which a glossy surface appeared on the sliding plate. The multicyclic characteristics based on this study clearly differed from those of the conventional study in their fluctuation range and recovery between sets.

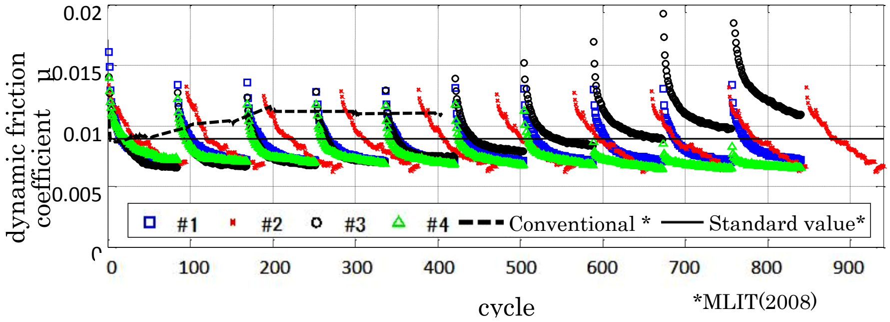

Figure 3.7 Friction coefficient variation

Fig. 3.8 shows the relationship between the temperature at the center of the sliding plate and the number of loading cycles for each specimen and set. For the purpose of measuring temperatures, thermocouples were attached to the backside of the sliding plate (SUS304, t6) through a hole in the steel backing plate. The figure shows a remarkable increase in temperature for each set, and some correlation is assumed between the increase in temperature and the decrease in friction, as well as between the initial temperature and the initial friction in Specimen #4.

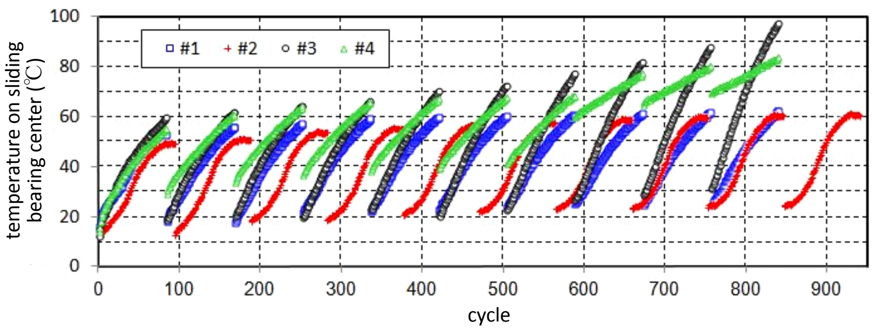

Figure 3.8 Temperature variation at the center of the sliding plate

4. CONCLUSIONS

In the high-friction sliding bearing tests, the temperature of the specimen increased, and the friction coefficient decreased according to the loading cycles. The trend of fluctuation of friction correlated well with the temperature of the sliding plate and bearing, cumulative absorbed energy, or cumulative sliding displacement.

The test results of the low-friction sliding bearings showed that their friction fluctuation was extremely small even when the axial pressure was 1.5 times the standard value, and they demonstrated sufficient stability under multicyclic loading. However, the trends of friction fluctuation, such as in terms of the fluctuation range or recovery, that were observed in the tests, could not be expressed through conventional estimation.

Consequently, both types of sliding bearings were found robust against multicyclic loading under an axial pressure of 20 MPa and cumulative displacements of 50 m which were derived from the response to a long-period earthquake motion.

ACKNOWLEDGEMENT

This paper describes a portion of the results of the promotion project for building-standards maintenance “27-3 Examination about the safety verification method of the seismic isolated buildings against long-period ground motions,” conducted by the Ministry of Land, Infrastructure, Transport and Tourism in the Heisei 22 fiscal year.

Gratitude is respectfully expressed to the main committee (Chairperson: Professor Haruyuki Kitamura of Tokyo University of Science), WG for the testing of devices (Chief examiner: Professor Mineo Takayama of Fukuoka University), WG for the evaluation of the response of buildings (Chief examiner: Professor Takeshi Furuhashi of Nihon University), and all the persons concerned.

REFERENCES

Shimizu Corporation, Kobori Research Complex Inc. and Japan Society of Seismic Isolation (2010). Examination on Maintenance of Standard for Seismic Isolated Structures (in Japanese). The Report in the Heisei 21 Fiscal Year on Building-Standards Maintenance Promotion Project of Ministry of Land, Infrastructure, Transport and Tourism. **No.12:** 4.1-32-4.1-36.

Hibino, H. et al. (2003). Modeling of Friction Characteristics of Elastic Sliding Bearing based on Loading Test using Full Scale Specimen (in Japanese). *Journal of Structural and Construction Engineering, Transactions of AIJ* .**574,** 45-52.

Ministry of Land, Infrastructure and Transport (2008) . An Attached Table of Building-Materials Verification Document for Oiles Type Sliding Bearings (in Japanese). **MVBR-0377**

Hamazaki, H. et al. (2007). The experimental study about durability ability of the elastic sliding bearing : Part 2 The experiment result of the low and high friction type elastic sliding bearing (in Japanese). *Summaries of technical papers of Annual Meeting Architectural Institute of Japan 2007.* B-2, **Structures II:** 1061-1062.